# Ghost Spectra and Rubbish Electrons in a CMA

N. Nissa Rahman , K. Goto, and R. Shimizu*

*Nagoya Institute of Technology, Gokiso-cho, showa-ku, Nagoya 466-8555, Japan*
*\*Osaka Institute of Technology, Kitayama 1-79, Hirakata 573-0196, Japan*

The ghost spectra and rubbish electrons due to the scattered electrons in a CMA were examined. The major ghost spectrum observed at about 5% higher energies were yielded at the edge of the other side of the annular slit just before the detector. Accordingly, we set an extra baffle slit to cut down the extraneous electrons between the slit and the exit mesh of the CMA. The reduced (by a factor of 10) ghost spectrum of less than $10^{-4}$ was obtained in our novel CMA. Those electrons of energies lower than the normal spectrum through the secondary electrons were roughly obtained by Seah's method by biasing the sample to reflect the incoming electrons. Broad ghost like and rubbish electrons were found over the energy range, though these were the order of $10^{-5}$ and below, respectively. The scattered electrons at the mesh seemed to slightly broaden the spectrum. The onset of the ghost secondary electrons at "0-eV" would show the approximate rubbish electron level (*i.e.*, background) of the whole spectra.

## 1 Introduction

We are making a data base for the VAMAS (Versailles Project on Advanced Materials and Standards)-SCA (Surface Chemical Analysis) project of Common Data Processing (Compro) in Japan and preparing for the work in the ISO/TC201 (on Surface Chemical Analysis) SC5&7 ('5 for Auger electron spectroscopy: AES and '7 for X-ray photoelectron spectroscopy: XPS). This database should be in a manner of metrology and thus be **SI** traceable. For this work a novel cylindrical mirror analyzer (CMA) of AES (Auger electron spectroscopy) analyzer has been developed [1] and improved [2]. The design is quite identical to that of by Varga *et al* [3], which uses naturally formed ideal logarithmic electrostatic potentials between two concentric cylinders having gaps at both ends, Fig. 1.

The analyzer shall be free from any artifacts (spectrum-like ghost and background-like rubbish electrons) which are the scattered electrons in the analyzer. The artifacts do exist in an actual analyzer, so that this has to be decreased as small as possible to the level of detection limits. We aimed this level well below 0.1% of the spectrum but the values of 0.1~1% will be acceptable in a conventional AES according to the stability and noise level. The endeavors to reduce the artifacts have been made by many authors, which are to blacken the surface with soot, aquadag (mixture of carbon), porous gold black [4] , rough figured materials, and/or effective baffles to cut or to absorb these electrons. Froitsheim *et al* used the corrugated deflectors in the 127° type analyzer and reduced the ghost by a factor of 10 or more [5]. They also discussed the use of deflectors with woven mesh [4] to let escape the electrons hitting onto it and concluded that this method was not so effective. Further they recommended to use the saw tooth corrugation in a CMA and photoemission spectroscopy. Bargeron and Nall observed the artifact in CMA, which is the electrons scattered at the inner cylinder [6]. Seah observed the artifacts in the hemispherical analyzer using quasi elastically scattered electrons [7,8]. El Gomati and El Bakush simulated the electron scattering in a CMA and found the most dominant source of the artifacts can be the edge of the detection slit just before the detector [9]. We improved our CMA after the last reference and this has been of significance.

This paper is a modified version of the paper presented at the 3rd Korean-Japan International Symposium on Surface Analysis [10]. More details and general description are given.
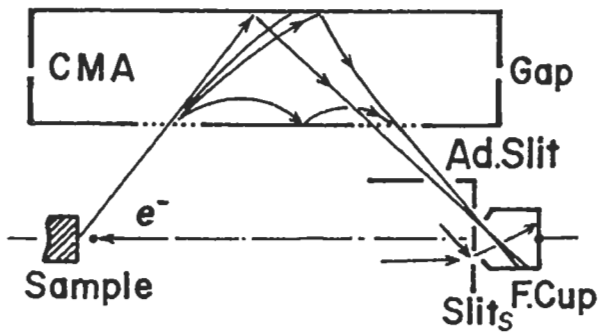
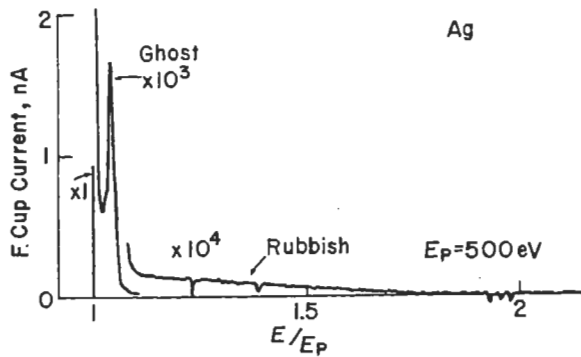Fig. 1 Scattered electrons that could be observed in CMA.



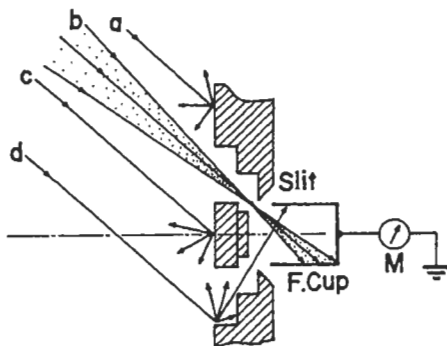Fig. 2 The major ghost and rubbish electrons observed in the prototype.



Fig. 3 Schematic geometry of the annular slit and Faraday cup. The ray (d) would generate the ghost.
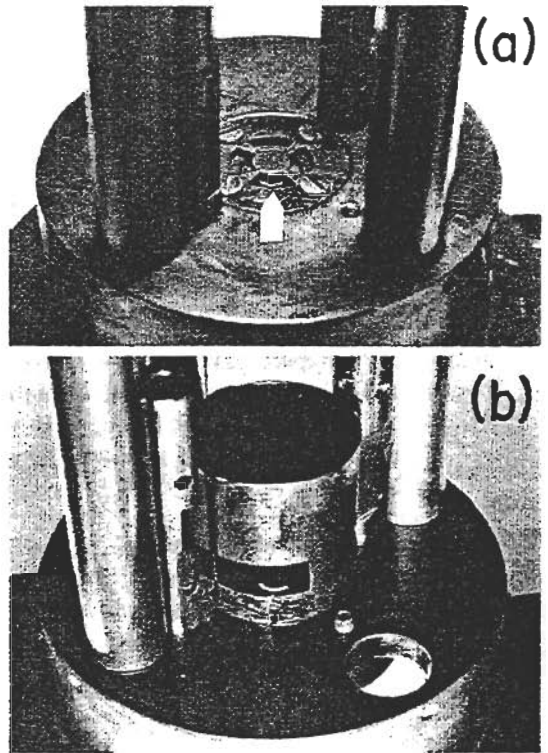


Fig. 4 Photographs of slit; (a) prototype, arrow shows the slit, and (b) with an additional baffle slit.
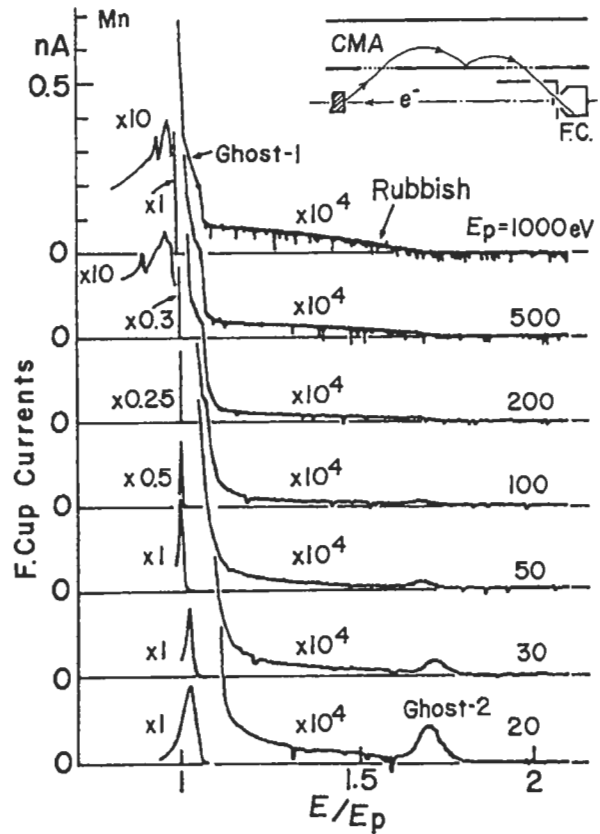


Fig. 5 Ghost and rubbish electrons in the higher energy range.

field. Elastically backscattered primary electrons (BS) were used as a sample spectrum to study the ghost and rubbish electrons. The scattered electrons that could be observed in the CMA are schematically shown in Fig. 1. In the prototype the generation of major ghost and rubbish spectra observed at just above the BS is shown in Fig. 2 and it amounted to be 0.1~0.2% of BS in height [1]. The possible cause of this ghost is schematically shown in Fig. 3. The electron beam **a, b,** and **c** are for the corresponding sweeping energies of lower, normal, and higher ones, respectively. Little scattered electrons would enter into the Faraday cup (detector). While the sweeping energy considerably passes through the normal energy (**b**) and hits the other side of the annular slit (**d**), a fraction of the scattered electrons can get into the Faraday cup. The effect can be greatest because the beam is almost focused and the solid angles for the detector is considerably large. This would be observed as an artifact *i.e.*, the ghost. This kind of ghost may not be found in the single hole slit. To cut this beam of **d**, an additional baffle slit was set as is shown in Figs. 1 and 4. Fig. 4 shows two photographs of prototype (**a**), the arrow showing the slit, and that with an additional baffle slit (**b**) over the prototype. In Fig. 5, the ghost and rubbish electrons being observed with the baffle slit are shown. The primary electron currents were about $0.4 \mu$ A. The ghost-1's do not show the clear feature, while it was spectrum-like before the improvements (Fig.2). The height is of the order of $10^{-4}$ of the main spectrum and fades for the lower primary energies. This value is an factor of 10 or more smaller compared with the former case of without the additional baffle slit [1]. The ghost-2's are found at about 1.7 times of higher energies of the primary electrons, which increase as the primary energy decrease, because the fraction of the ratio of BS increases. The ghost-2's are the elastically scattered BS at the inner cylinder once [6]. Higher order of scattering and reflection were not observed. The scattered electrons in the inner cylinder would practically be absorbed on the second scattering.

In the above experiments the ghost and rubbish electrons in the range between 0-eV and the spectrum could not be obtained, though it is of the most pertinent range where actual AES spectra would appear. Then we employed the Seah's quasi-elastically reflected primary electron method [7,8], which biases the sample at almost the accelerating voltages of primary electrons and thus can reflect the incident primary electron beam without interacting with sample. The primary beam should make an imaginary focus on the sample, but it was hardly attainable. Although this method would closely simulate an actual situation. Obtained results for the primary electron energies of 500eV and 100eV are shown in Figs. 6, (**a**) and (**b**), respectively. Two figures are similar in quality. The characteristics of (**a**) in the higher energies($>$BS) are quite similar to the former case in Fig. 5. The onset ① reflects the so called secondary electrons emitted at the outer cylinder and will be discussed later. The ghosts ② and ③, and rubbish electrons are observed. The ghost ③ is too broad for the spectrum and still in the order of $10^{-5}$. The broader ghost can easily be distinguished from the real spectrum but not from the background. These ghosts could be generated at the outer cylinder; the slightly curved rays in the Fig. 1. These scattered electrons from an outer cylinder may completely be reduced with large enough radius 3.44 of the internal cylinder, shown in Fig. 7; ours being 2.4 and conventional ones being ~2.2. The value of 3.44 of outer cylinder, however, is not practical with too much of empty space. We should optimize the structure considering the other overwhelmingly large noises and fluctuations. For the outer cylinder of 3.71, the sweeping energy equals the actual voltage applied. The energy width of BS ④'s seems too broad for the thermal spread of the BS and energy resolution of the CMA. This is due to the broad primary beam that would imaginary focus on the sample.

The onset of secondary electrons in Figs. 6, (**a**) and (**b**), ①'s would show the secondary and scattered electrons at the outer cylinder without receiving a sweeping voltage, then thus travel directly to the Faraday cup. This is

## 2. Experiments and Discussion

We used our novel CMA which has been improved from the prototype [1] and incidentally a poly-crystal of Mn as a target sample. In the CMA the surfaces that electrons would hit were coated with aquadag and/or soot of butane gas to reduce the electron scattering. The thickness of the coatings should be kept uniform within $10\mu$ m in the CMA to maintain the designed electrostatic field. Elastically backscattered primary electrons (BS) were used as a sample spectrum to study the ghost and rubbish electrons. The scattered electrons that could be observed in the CMA are schematically shown in Fig. 1. In the prototype the generation of major ghost and rubbish spectra observed at just above the BS is shown in Fig. 2 and it amounted to be 0.1~0.2% of BS in height [1]. The possible cause of this ghost is schematically shown in Fig. 3. The electron beams **a, b,** and **c** are for the corresponding sweeping energies of lower, normal, and higher ones, respectively. Little scattered electrons would enter into the Faraday cup (detector). While the sweeping energy considerably passes through the normal energy (**b**) and hits the other side of the annular slit (**d**), a fraction of the scattered electrons can get into the Faraday cup. The effect can be greatest because the beam is almost focused and the solid angles for the detector are considerably large. This would be observed as an artifact *i.e.,* the ghost. This kind of ghost may not be found in the single hole slit. To cut this beam of **d**, an additional baffle slit was set as is shown in Figs. 1 and 4. Fig. 4 shows two photographs of prototype (**a**), the arrow showing the slit, and that with an additional baffle slit (**b**) over the prototype. In Fig. 5, the ghost and rubbish electrons being observed with the baffle slit are shown. The primary electron currents were about $0.4\mu$ A. The ghost-1's do not show the clear feature, while it was spectrum-like before the improvements (Fig.2). The height is of the order of $10^{-4}$ of the main spectrum and fades for the lower primary energies. This value is a factor of 10 or more smaller compared with the former case of without the additional baffle slit [1]. The ghost-2's are found at about 1.7 times of higher

energies of the primary electrons, which increase as the primary energy decrease, because the fraction of the ratio of BS increases. The ghost-2's are the elastically scattered BS at the inner cylinder once [6]. Higher order of scattering and reflection were not observed. The scattered electrons in the inner cylinder would practically be absorbed on the second scattering.

In the above experiments the ghost and rubbish electrons in the range between 0-eV and the spectrum could not be obtained, though it is of the most pertinent range where actual AES spectra would appear. Then we employed the Seah's quasi-elastically reflected primary electron method [7,8], which biases the sample at almost the accelerating voltages of primary electrons and thus can reflect the incident primary electron beam without interacting with sample. The primary beam should make an imaginary focus on the sample, but it was hardly attainable. Although this method would closely simulate an actual situation. Obtained results for the primary electron energies of 500eV and 100eV are shown in Figs. 6, (**a**) and (**b**), respectively. Two figures are similar in quality. The characteristics of (**a**) in the higher energies($>$BS) are quite similar to the former case in Fig. 5. The onset ① reflects the so called secondary electrons emitted at the outer cylinder and will be discussed later. The ghosts ② and ③, and rubbish electrons are observed. The ghost ③ is too broad for the spectrum and still in the order of $10^{-5}$. The broader ghost can easily be distinguished from the real spectrum but not from the background. These ghosts could be generated at the outer cylinder; the slightly curved rays in the Fig. 1. These scattered electrons from an outer cylinder may completely be reduced with large enough radius 3.44 of the internal cylinder, shown in Fig. 7; ours being 2.4 and conventional ones being ~2.2. The value of 3.44 of outer cylinder, however, is not practical with too much of empty space. We should optimize the structure considering the other overwhelmingly large noises and fluctuations. For the outer cylinder of 3.71, the sweeping energy equals the actual voltage applied. The
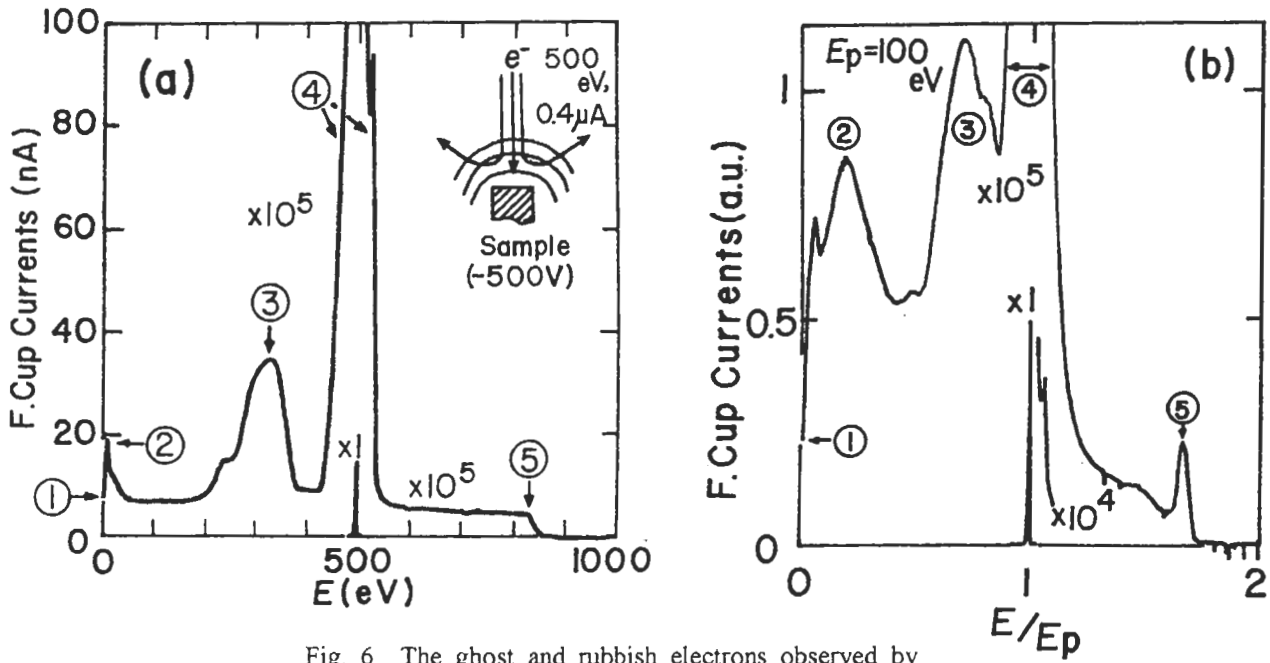
Fig. 6   The ghost and rubbish electrons observed by using quasi-elastically reflected primary electrons.
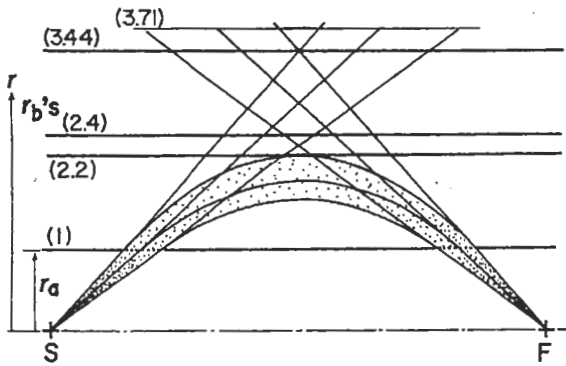


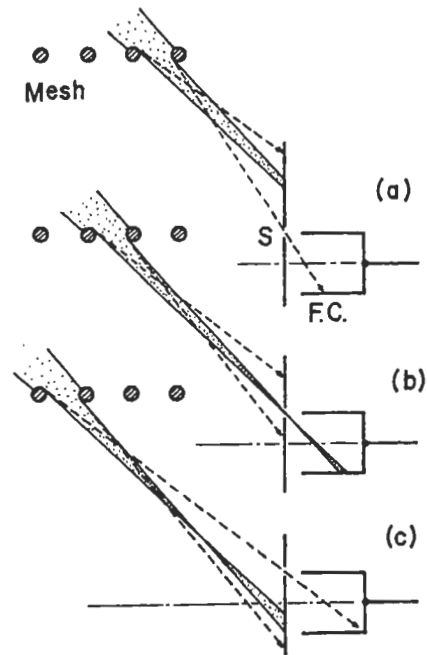Fig. 7   Design of outer cylinder radii.



Fig. 9   Schematic rubbish electrons from the exit mesh. Solid lines are normal electron traces and broken ones are rubbish electron
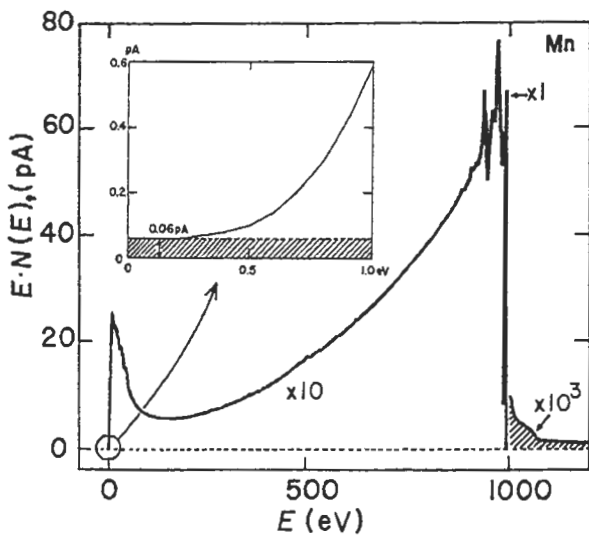


Fig. 8 Typical example of   a whole energy distribution of   Mn   at 1000eV. The blow-up of the onset of the SE is shown in the inset.

9. M.M.El Gomati ang T.A.El Bakush, Surf. Interface Anal. **24**, 152 (1996).
10. K. Goto, N. Nissa Rahman, and R. Shimizu, in *3rd Korean-Japan International Symposium on Surface Analysis* (Kyong Ju, Korea, Nov. 2-3, 2000).

## Reviewer's Comments and Questions

Reviewer: Tetsu Sekine (JEOL)

The paper revealed the very fine characteristic of CMA, which would be the essential knowledge to the measurement of higher precision, and also described the improvement of CMA capability by authors. I recommend publishing with minor revision.

Q1) In figures 2 and 5, the elastic electrons from Mn poly-crystal specimen is used for evaluating the fractions of ghost peak and background, the both are the artifact generated by the scattered electrons in CMA. Is there any particular reason for employing Mn specimen?
A1) It was quite incidental, but Mn is suitable since the atomic number is rather intermediate.

Q2) I think that figure 6 is a good data indicating that the different scattering processes are taking place in CMA. Could you give any interpretation why the scattered electrons and secondary electrons, which are generated at the outer cylinder, forms ghost peaks at two locations, ② and ③, as shown in figure 6?
A2) The ghost is due to the secondary and scattered electrons directly from the outer cylinder almost without receiving a sweeping voltage on it, so that their trajectories are almost straight. While that is due to those electrons received the sweeping voltage, then their traces might be curved. They are shown schematically in Fig.1, but we can't give any reasonable shape as it is very complicated phenomenon.

Q3) Regarding data in figure 5, as the authors have already pointed out, the elastic peaks are broad. Broadening is more remarkable at lower primary energies, such as roughly 22 eV at Ep=20 eV from the chart. Is there any possibility that the cause of broadening is due to the expansion of signal source size? How much is the primary beam size under Ep=20 eV?
A3) The beam size was about 1-mm at FWHM. The increased likely broadening in the lower Ep's is not an actual broadening but the inherent thermal energy spread of the primary beam. Some "rubbish" are, of coarse, included in it.
Q3') The beam size at 20 eV is about 1 mm in diameter. Then, it will not be the factor inducing the large peak broadening such as 22 eV.
A3') The broadening is 1.5eV at most, which includes effects of the thermal, instrumental lens, work function. It seems too much broadening but it is reasonable by considering the magnification and normalized-scale.

Q4) The authors have explained that the broadening of Mn elastic peaks in figure 5 is due to the "so-called rubbish electrons" scattered at the exit mesh of inner cylinder. Are these the scattered primary electrons or the secondary electrons? If it is the former, the effect should appear similarly at any range of Ep in the current vs. E/Ep expression. If it is the latter, the effect will be more smoothed against energy sweep in contrast with the case described in figure 3, because they will not focus sharply. In other word, the reviewer thinks that the rubbish electrons cannot interpret the broadening phenomena. Therefore, I recommend reconsideration for the final paragraph of section 2 (from 14th line to 35th line from the top in the left column at page 5).
A4) We can't separate the scattered and the secondary electrons, then they are said as "rubbish". The broadening excepting the ghost is considerable when we observed the elastic peaks in detail. (We don't change the description.)
Q4') If the rubbish electrons generated at the exit mesh were the main or second cause of broadening, then it must be a "ghost like peak" which is comparable order with the elastic peak in shape and in intensity. If so, convolution of the elastic peak with it can

make broadening of the observed level.   If not, in other words, very broad and weak, then it will appear like a background. In Fig.5, broadening is remarkable below 50 eV. Over 50 eV, it is not visible on the chart. The supposed "ghost like peak" must effective below 50 eV, but not much over 50 eV. I wonder that the rubbish electrons generated at the exit mesh would have the feature of "ghost like peak" mentioned above.

A4') The phenomenon is very complicated and can't easily be resolved. But it should be noted that the steradians and directions for the scattered electrons at the exit mesh to the detecting slit are strictly limited, then thus bery small fraction of the scattered lectrons would appear as broadenig rubbishes. In general the elastcally scattered electrons would increase in the lower range of Ep.

Q5) Regarding figure 9, an explanation about the meaning of lines, solid and dot, should be given. Are these computer-generated lines or just showing the concept?

A5) The lines are conceptual ones. (We add explanation in the caption; Fig.9.)

Some abbreviations and their explanations have been corrected  and/or added according to the comments form reviewers, T. Sekine (JEOL) and A. Tanaka (ULVAC-PHI).